Journal of Applied Physics ARTICLE pubs.aip.org/aip/jap

A cesium-iodide surface treatment for enhancement of negative electron affinity photocathode chemical robustness

Cite as: J. Appl. Phys. **137**, 224901 (2025); doi: 10.1063/5.0271931
Submitted: 20 March 2025 · Accepted: 26 May 2025 ·
Published Online: 9 June 2025

S. J. Levenson,[1,a)] M. B. Andorf,[1] M. A. Reamon,[1] I. V. Bazarov,[1] A. Galdi,[2] Q. Zhu,[3] M. A. Hines,[3] J. Encomendero,[4] V. V. Protasenko,[4] D. Jena,[4,5,6] H. G. Xing,[4,5,6] and J. M. Maxson[1]

AFFILIATIONS

[1]Cornell Laboratory for Accelerator-Based Sciences and Education (CLASSE), Cornell University, Ithaca, New York 14850, USA
[2]Department of Industrial Engineering, University of Salerno, Fisciano (SA) 84084, Italy
[3]Department of Chemistry, Cornell University, Ithaca, New York 14853, USA
[4]School of Electrical and Computer Engineering, Cornell University, Ithaca, New York 14853, USA
[5]Department of Material Science and Engineering, Cornell University, Ithaca, New York 14583, USA
[6]Kavli Institute at Cornell for Nanoscale Science, Cornell University, Ithaca, New York 14583, USA

[a)]**Author to whom correspondence should be addressed:** sjl354@cornell.edu

ABSTRACT

Photocathodes activated to negative electron affinity with a cesium-based activation layer, such as GaAs and GaN, can be used for generating spin-polarized electron beams, but their extreme sensitivity to chemical poisoning limits their operational lifetimes. This work demonstrates that applying and subsequently heating a cesium iodide (CsI) coating can produce a more durable activation layer lacking iodine, but rich in stable cesium suboxides (formal O oxidation state > -2), which significantly extend the dark lifetimes of both GaAs and GaN photocathodes. Through x-ray photoelectron spectroscopy, we examine the stability and formation of these Cs suboxides, which exhibit remarkable resistance to chemical poisoning. Additionally, we investigate the subsequent surface quality using atomic force microscopy. Our findings show that CsI-based surface treatments not only prolong photocathode lifetime but also maintain high spin polarization, positioning this method as a promising approach for enhancing photocathode durability in demanding applications.

I. INTRODUCTION

Spin-polarized electron beams are essential in nuclear and particle physics and electron microscopy. Currently, gallium arsenide (GaAs) is the only material utilized as a spin-polarized photoemission source. Facilities like the Continuous Electron Beam Accelerator Facility (CEBAF)[1] at Jefferson Laboratory and the Mainz Microtron (MAMI)[2] use GaAs photocathodes to study the internal structure of nucleons and strong nuclear forces. As future facilities like the International Linear Collider (ILC)[3] and Electron-Ion Collider (EIC)[4] are developed, the demand for robust, highly polarized electron sources will grow. Furthermore, the integration of GaAs photocathodes into spin-polarized electron microscopes drives progress in understanding spin-related properties at the microscopic level, enabling studies of magnetic properties and spin-dependent phenomena at the nanoscale.[5–7]

Spin-polarized photoemission[8,9] involves exciting electrons from the top of the valence band using circularly polarized photons with energy near the material bandgap. For efficient photoemission, GaAs is operated in or near a negative electron affinity (NEA) state where if an electron initially at the top of the valance band absorbs a photon having an energy equivalent to the material's bandgap energy, it will be excited to the bottom of the conduction band and be emitted if it reaches the GaAs surface.[10] Bulk NEA GaAs is theoretically limited to a maximum electron spin polarization (ESP) of 50% while typical experiments measure around 35%–40% due to various depolarization mechanisms that occur in transit through

the material.[11–14] Strained superlattice GaAs can overcome this limitation by achieving spin polarizations exceeding 90%.[15]

To activate a GaAs photocathode to NEA, an electric dipole moment is induced on the surface by depositing an electropositive metal, cesium (Cs), with an oxidizing agent such as oxygen or NF_3. However, the chemical reactivity of Cs and its susceptibility to oxidation significantly compromise the operational lifetime of NEA GaAs, confining its application to ultrahigh vacuum environments and only to direct current (DC) injectors,[16,17] though a program to develop a radio-frequency (RF) gun with a GaAs electron source has made considerable progress.[18] This limitation has spurred interest in developing spin-polarized electron sources with longer operational lifetimes. Photocathodes such as CsTe[19,20] and Cs_3Sb[21,22] are known to have operational lifetimes greatly exceeding that of GaAs. Interestingly, these materials have also been used to generate a more chemically robust NEA activation layer for both bulk and superlattice GaAs photocathodes.[23] Other materials capable of producing spin-polarized electrons have also been investigated.[24] A recent result indicates that a durable alkali-antimonide Na_2KSb photocathode could produce spin-polarized beams.[25] Additionally, spin-polarized photoemission from gallium nitride (GaN), both in its zinc blende and wurtzite phases, has been demonstrated.[26] GaN may achieve NEA with only Cs and no oxidant and has been shown to have a longer dark lifetime than NEA GaAs.[26,27]

Another Cs-based material utilized as a robust photoemitter is cesium iodide (CsI) which has remarkable durability and stability.[28–33] It exhibits little sensitivity to chemical poisoning from most common residual gas molecules found in vacuum systems, with the exception of water vapor. CsI has been particularly successful as a photoemitter in Ring Imaging CHerenkov (RICH) detectors,[34] where it demonstrates outstanding resilience to air exposure while achieving quantum efficiencies (QEs) exceeding 50% with incident far-ultraviolet light.[35,36]

Although its relatively high work function prohibits its use as an emitter material in photo-injectors, CsI has been used to lower the work function of metal photocathodes[37] and enhance the performance of carbon fibers for field emission beam production.[38] CsI has also been investigated as a coating layer for alkali-antimonide photocathode materials.[30,39,40]

In this work, we investigate the use of CsI as a component in producing a more robust NEA layer for both GaAs and GaN photocathodes. The paper is structured as follows. In Sec. II, we detail the preparation of samples used, followed by their activations with Cs in Sec. III. In Sec. IV, we describe spin-polarization measurements on GaAs samples activated to NEA. Section V deals with the surface analysis performed on CsI-treated samples, including atomic force microscopy (AFM) and x-ray photoelectron spectroscopy (XPS) data. This is followed by a discussion (Sec. VI) and a conclusion (Sec. VII).

II. SAMPLE PREPARATION

For GaAs, single crystal (100, Zn-doped, carrier concentration $9 \times 10^{18}\,cm^{-3}$) wafers acquired from AXT-Tongmei, Inc. were cut to $1 \times 1\,cm^2$ samples with a diamond scroll. A chemical etch to remove surface oxidation was performed on the samples, which included ultrasonication in isopropanol, followed by a de-ionized (DI) water rinse, a 30 s immersion in a 1% HCl solution, and a final rinse with DI water. Samples were dried and sealed in bags pressurized with dry nitrogen.

For GaN, samples were grown in a Veeco Gen10 molecular beam epitaxy (MBE) system at Cornell University. A 1 μm Mg-doped p-GaN layer with a doping concentration of $3 \times 10^{19}\,cm^{-3}$ was deposited epitaxially using step-flow growth mode in metal-rich conditions. The GaN films possessed a Ga-polar hexagonal wurtzite structure oriented along the (0001) plane. A GaN template on sapphire was used as the substrate and was prepared with ultrasonication for 10 min each in acetone, methanol, and isopropanol, followed by degassing at 200 °C for 7 h in vacuum. Photoemission properties of similarly prepared GaN samples have been reported previously.[41] After growth, each sample was transferred under static vacuum to the Cornell Photocathode Laboratory[42] for subsequent analysis.

All samples were fixed to a stainless steel puck. For thermal and electrical contact, indium foil was placed between the sample and the puck. The assembly was then placed in a UHV growth chamber (base pressure 5×10^{-10} Torr as read by a cold cathode gauge), featuring a quartz micro-balance (QMB), a SAES Cs dispenser filament source, an evaporative effusion cell containing 99.999% pure CsI metal beads (Sigma-Aldrich Chemical Corporation), and an electrical feedthrough for biasing the photocathode. Photoemission measurements used an NKT Photonics SuperK Extreme monochromated supercontinuum visible light source (10 nm bandwidth light tunable between 400 and 800 nm wavelength) as the incident light, unless otherwise noted.

III. ACTIVATION WITH Cs AND CsI TREATMENT

Once in vacuum, the samples were heated at approximately 600 °C for 6 h. During activation, Cs was applied to the surface of the samples while the photocathode QE was monitored with either 10 μW of 532 nm light for GaAs or a 10 μW 265 nm light emitting diode (LED) for GaN. Cs deposition ended when a peak in the QE was observed. After deposition, the QE was monitored to measure the dark lifetime as shown in blue in Figs. 1 and 2.

After the lifetime measurement, the photocathode was again heated at 600 °C for 6 h. Subsequently, a CsI layer was grown on the photocathode surface. During the growth, the CsI effusion cell was heated to 500 °C, while the photocathode was held at 150 °C. The CsI deposition rate was monitored with the QMB until 1 nm was deposited. The photocathode then underwent a second cesiation and lifetime measurement, as shown in orange in Figs. 1 and 2. Following this lifetime measurement, two more cycles of heating (600 °C for 6 h), cesiation and lifetime measurements were performed without further CsI deposition (yellow and blue curves in Figs. 1 and 2, respectively).

Since it was observed (shown in Fig. 3) that consecutive heating cycles can increase the dark lifetime, another GaAs photocathode, prepared the same way, was given four consecutive cycles of cesiation, dark lifetime measurement and 6 h 600 °C heating without CsI deposition between cycles 1 and 2. The obtained dark lifetimes are shown in blue in Fig. 3. After four cycles, we see a factor of 5 improvement in the dark lifetime. For comparison, the

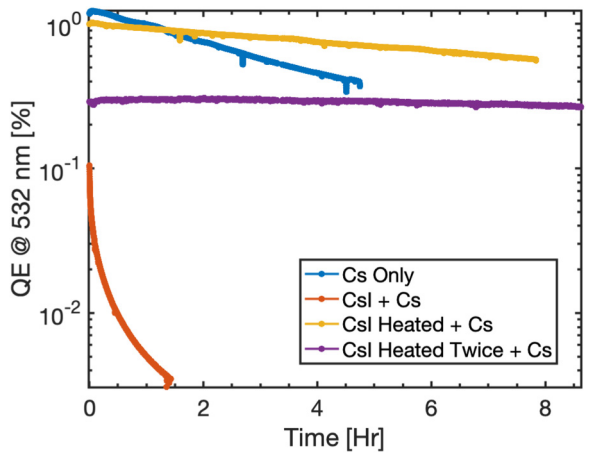

FIG. 1. Lifetime measurements of the GaAs photocathode at various stages under identical vacuum conditions (5×10^{-10} Torr). The lifetime after the initial cesiation is shown in blue. An exponential fit produces a $1/e$ lifetime of 4.2 h. The lifetime after deposition of 1 nm of CsI and subsequent cesiation is shown in red and the $1/e$ lifetime from an exponential fit was found to be 0.6 h. After heating the CsI layer and cesiating again, the lifetime is shown in yellow and the $1/e$ lifetime from an exponential fit was found to be 14.1 h. The lifetime after another heating cycle and cesiation is shown in purple, where the $1/e$ fit is 77 h.

lifetimes from the activations in Fig. 1 are also plotted in Fig. 3, demonstrating the factor of 18 improvement in lifetime, thus decoupling the enhancement from consecutive heating cycles with the enhancement seen from CsI deposition. During all lifetime measurements, the base pressure in the chamber was maintained at 5×10^{-10} Torr. The chamber was not vented between lifetime measurements in order to compare the photocathode lifetimes in the same vacuum conditions.

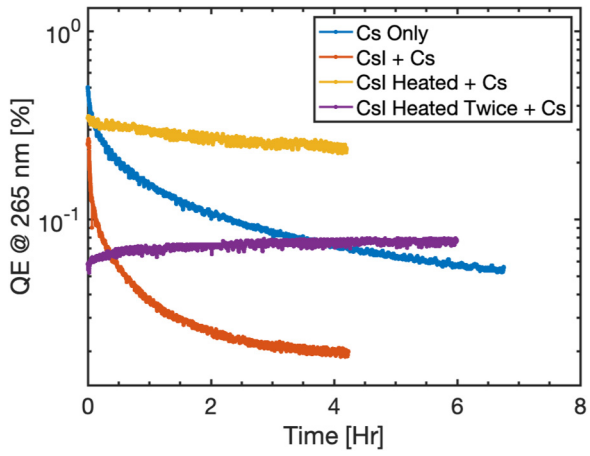

FIG. 2. Lifetime measurements of the wurtzite GaN photocathode at various stages under identical vacuum conditions (5×10^{-10} Torr). The lifetime after the initial cesiation is shown in blue. An exponential fit yielded a $1/e$ lifetime of 4.6 h. The lifetime after deposition of 1 nm of CsI and subsequent cesiation is shown in red and the $1/e$ lifetime from an exponential fit was found to be 2.9 h. After heating the CsI layer and cesiating again, the lifetime is shown in yellow and the $1/e$ lifetime from an exponential fit was found to be 13.6 h. The lifetime after another heating cycle and cesiation is shown in purple, where the QE slightly increases over 6 h.

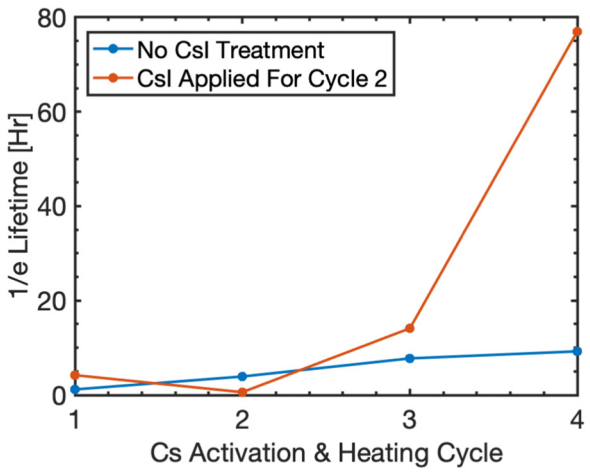

FIG. 3. A comparison between the dark lifetimes of a GaAs photocathode with repeated cesiation + heating cycles, and the photocathode described in Fig. 1.

IV. GaAs STUDIES FOR SPIN POLARIZATION

Since GaAs photocathodes are primarily used as spin-polarized electron sources, parameters relevant to spin-polarized operation were investigated. For this, GaAs photocathodes were activated with Cs and NF_3 to fully achieve the NEA state. One sample underwent the activation procedure detailed above (6 h heating, cesiation, 6 h heating, 1 nm CsI layer deposition, 6 h heating, cesiation, and 6 h heating) and another sample was heated for 24 h at 600 °C for comparison. In order to incorporate NF_3 into the activation layer, the samples were transported in vacuum to a separate chamber outfitted with both a Cs dispenser and a gas leak valve where they could be activated to NEA with sequential deposition while the QE was monitored with 780 nm light. There, the samples were activated to NEA with sequential deposition of Cs and NF_3, while the QE was monitored with 780 nm incident light. The sequential activation procedure started with depositing Cs as described above until the QE peaked. At this point, the Cs was turned off and a partial pressure of around 1 nTorr of NF_3 was leaked in the chamber until the QE dropped by 1–2 orders of magnitude. The NF_3 leak valve would then be closed and the Cs turned back on, bringing the QE to a higher peak than before. This process was repeated several times until saturation. The NEA activations are shown in Fig. 4. Note the GaAs photocathode with no CsI took about twice as long to achieve a peak QE as did the CsI-treated one.

Upon activation to NEA, the photocurrent was monitored for several hours, as shown in Fig. 5. The dark lifetime of the CsI-treated photocathode was measured to be 13.3 times that of the

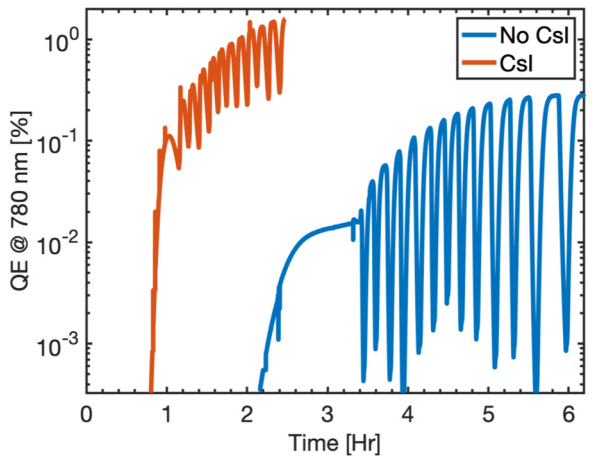

FIG. 4. A comparison of the Cs-NF_3 activations with 780 nm incident light described in the text. In both cases, the Cs deposition started at time $t = 0$ h.

GaAs photocathode with no CsI, similar to the Cs-only activation layer result from above.

After the lifetime measurement, the photocathodes were activated to NEA as before. A spectral response QE measurement was performed, as shown in blue in Fig. 6. Next, the photocathodes were transported in vacuum to the retarding-field Mott Polarimeter so that the spin polarization of the photoemitted beam from each photocathode could be measured. For details on the Mott Polarimeter in the Cornell Photocathode Laboratory, see previous studies.[19,21,23,26] Measurements were done with incident light that

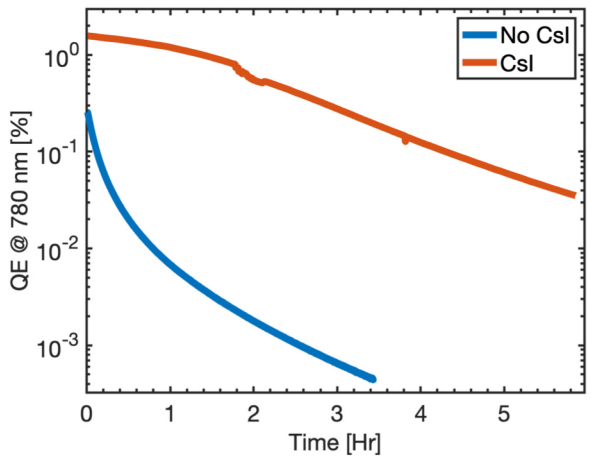

FIG. 5. A lifetime comparison with 780 nm incident light of a GaAs photocathode without CsI and a CsI-treated GaAs photocathode when activated to NEA with a sequential deposition of Cs and NF_3. The $1/e$ lifetime of the GaAs photocathode without CsI is 0.15 h and the $1/e$ lifetime of the CsI-treated photocathode is 2 h, a 13.3 times improvement.

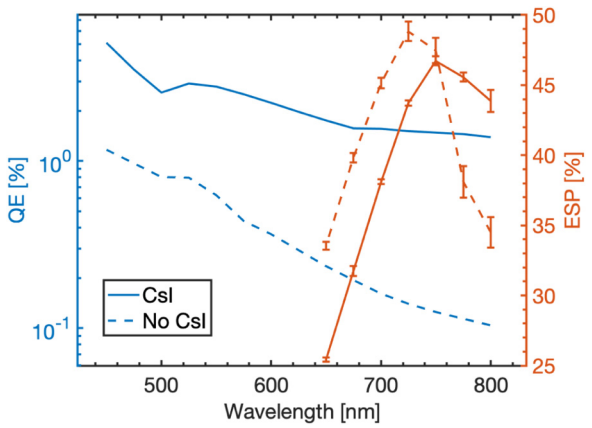

FIG. 6. The QE and ESP of both the GaAs without CsI and CsI-treated GaAs when activated to NEA with Cs + NF_3. The curves for the CsI-treated photocathode are solid and the curves for the GaAs with no CsI are dashed. The spin-polarization curve for the GaAs without CsI is shifted up in magnitude and down in wavelength due to its higher electron affinity when measured.[9]

was circularly polarized with a linear polarizer and $\lambda/4$ waveplate. Results from the spin-polarization measurements with the two photocathodes are shown in red in Fig. 6. While both photocathodes possess reasonably high ESPs, the curve of the GaAs without CsI is shifted slightly up in magnitude and down in wavelength as a result of its likely higher electron affinity when measured.[9]

V. ANALYSIS

In this section, we investigate the nature of the sample surface at various stages in the CsI activation process. This is done through atomic force microscopy (AFM) scans on GaAs samples to characterize the physical structure of the surfaces, as well as with x-ray photoelectron spectroscopy (XPS) to analyze the chemical composition of the surfaces.

A. AFM

To explore the mechanisms behind the changes in photocathode robustness, we performed AFM scans (in air) on GaAs samples. These were done on samples at each step in the CsI enhancement process, as shown in Fig. 7. Figure 7(a) shows the polished GaAs sample as received from the manufacturer to be very smooth with an RMS roughness of 197 pm, while the sample after etching, shown in Fig. 7(b) has a slightly increased surface roughness of 286 pm. In addition to increased roughness, HCl etching has been shown to create an As-rich surface on GaAs.[43] A 6 h 600 °C heating seems to only have marginal effects on the surface, as shown in Fig. 7(c), where the roughness is 272 pm. When a 1 nm average CsI layer is deposited, shown in Fig. 7(d), the surface of the photocathode features domains of CsI, which are several nm tall. The RMS roughness of this surface is 7.97 nm. However, after another 600 °C heating for 6 h, the quality of the surface is seemingly recovered, as the roughness is 191 pm, shown

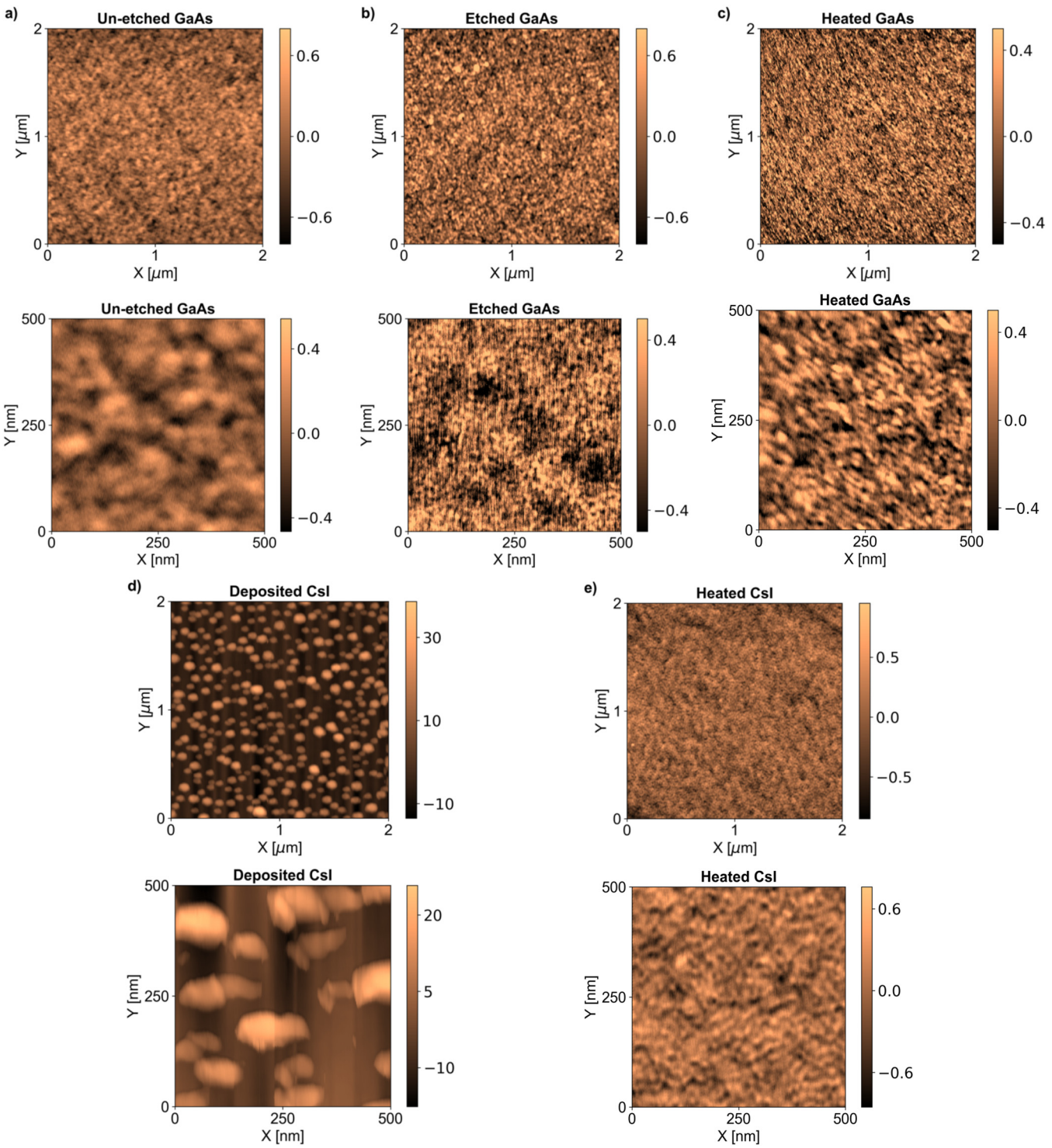

FIG. 7. GaAs photocathode AFM scans of $2 \times 2\,\mu m^2$ and $0.5 \times 0.5\,\mu m^2$ at different steps in the CsI enhancement process. GaAs sample shown are (a) as received after purchase, (b) after etching, (c) after a 6 h 600 °C heating, (d) after deposition of the 1 nm (as ready by the QMB) CsI layer, and (e) after another 6 h 600 °C heating. All colorbars have units of nm.

in Fig. 7(e). The observation of islands on the GaAs surface between deposition of CsI and heating likely explains the poor performance of the photocathode at this point. To better understand the lifetime enhancement observed after heating, we performed XPS to know the surface chemical composition.

B. XPS

After CsI deposition, XPS samples were exposed to air for approximately 5 min during transport to the XPS chamber. A GaAs sample coated with a 1 nm thick CsI film (no heating was done after CsI deposition) was loaded in the analysis chamber, then XP spectra were obtained using unmonochromated Al K_α radiation ($E_{\text{photon}} = 1486.7$ eV) and two different detection angles (0° and 70°) which probed regions 3 and 1 nm below the surface, respectively. After XP analysis, the sample was heated at 600 °C for 6 h, then XP analysis was repeated on the room temperature sample.

After analysis of the as-prepared and heated CsI/GaAs sample, the chemical stability of the heated sample was investigated. First, O_2 gas was introduced using a leak valve at 1×10^{-6} Torr for 125 and 625 s, corresponding to 125 L (Langmuir) and 625 L exposures, respectively. The sample was then exposed to 125 L and 625 L of H_2O (g). XPS analysis was performed after each exposure. To minimize the x-ray induced degradation of Cs oxides,[44] only O 1*s*, As 3*d*, and survey scans were obtained.

1. Chemical analysis of CsI/GaAs

Chemical analysis of the near-surface region of unheated, CsI-coated GaAs samples confirmed the presence of CsI and partially oxidized GaAs, as shown by the spectra in Fig. 8. The near-surface region was dominated by transitions assigned to CsI. This included the Cs $3d_{5/2}$ transition at 725.7 eV in Fig. 8(a), which we attributed[45] to Cs^+, and the I $3d_{3/2}$ and $3d_{5/2}$ transitions at 631.5 and 620.0 eV in Fig. 8(b), which we attributed[46] to I^-. Unoxidized GaAs was observed, as evidenced by Ga 3*d* photoelectrons at 19.5 eV and As 3*d* photoelectrons at 41.4 eV in Figs. 8(c) and 8(d), respectively. In contrast to the CsI transitions, the unoxidized GaAs transitions were more intense in normal detection than glancing detection, suggesting that these species were somewhat below the surface. Oxidized Ga and a tiny amount of oxidized As were also observed, as shown by the Ga 3*d* photoelectrons at 20.5 eV and As 3*d* photoelectrons at 44.7 eV, respectively. All Ga and As transitions were assigned in reference to Su *et al.*[47] The quoted photoelectron energies are only nominal energies, as band bending often produces small energy shifts ($\lesssim$0.2 eV) that may also be depth dependent. The nominal photoelectron energies are indicated by labeled dashed lines in all XP spectra.

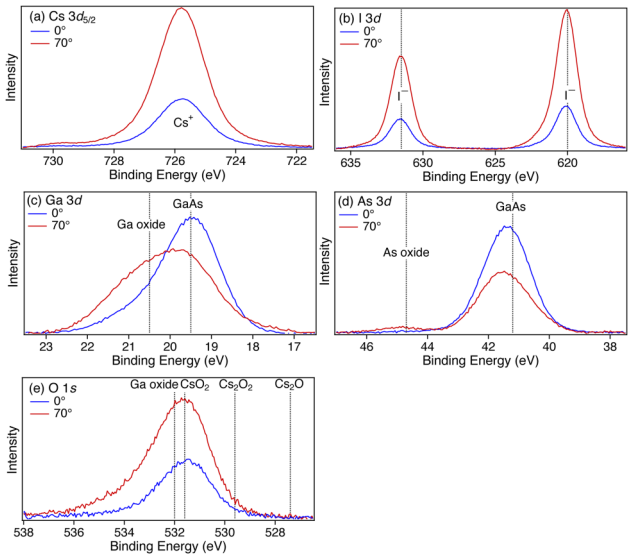

FIG. 8. X-ray photoelectron spectra of as-loaded CsI/GaAs observed with normal (0°, blue) and glancing (70°, red) detection, displaying the (a) Cs $3d_{5/2}$, (b) I 3*d*, (c) Ga 3*d*, (d) As 3*d*, and (e) O 1*s* transitions. Vertical dotted lines represent the nominal binding energies of the labeled species.

The presence of oxygen in the near-surface region of unheated, CsI-coated GaAs was somewhat unexpected, as the HCl etch was expected to remove any oxidized GaAs. The XP spectra showed that the oxidized species were localized in the near-surface region, as the O 1*s* transitions were more intense in glancing detection than normal detection. The XP spectra clearly indicated the presence of Ga oxides and the absence of I oxides. The presence of oxidized Cs compounds on the unheated substrates could not be ruled out. The oxidation chemistry of Cs is complex, consisting of peroxides, superoxides, and oxides. The vertical dotted lines in Fig. 8(e) represented the O 1s binding energies reported by Jupille *et al.* for CsO_2 (superoxide, 531.6 eV), Cs_2O_2 (peroxide, 529.6 eV), and Cs_2O (oxide, 527.4 eV).[48] Photoelectrons from oxidized gallium and CsO_2 have nearly identical energies and could not be distinguished.

XP analysis suggested that activation of the heated CsI-coated GaAs substrates was due to the formation of a cesium suboxide (formal O oxidation state > -2) surface layer. The XP analysis in Fig. 9 suggested that heating of CsI-coated GaAs led to desorption of I (presumably as I_2), (possibly partial) decomposition of Ga oxides, and formation of cesium suboxides, primarily Cs_2O_2. Heating removed all iodine species and oxidized As, as shown by the I 3*d* spectra in Fig. 9(b) and the As 3*d* spectra in Fig. 9(d). The intensity of the Ga oxide transition in the near-surface region, Fig. 9(c), was significantly reduced by heating. The identity of the Cs species after heating could only be inferred indirectly. The presence of metallic Cs could be definitively ruled out by the absence of plasmonic features in the Cs 3*d* spectra,[45] which implied that all Cs was in the +1 oxidation state and thus bound to oxygen. The production of cesium oxide, Cs_2O, can be definitively ruled out from the O 1*s* spectrum in Fig. 9(e). We concluded that after heating, cesium is primarily present as the superoxide, CsO_2; however, the presence of some cesium peroxide, Cs_2O_2, could not be ruled out.

2. Chemical stability of Cs suboxides

The chemical stability of the cesium suboxide-coated GaAs surface was investigated using increasingly large, sequential doses of O_2 and H_2O gases with intervening XP analysis, as shown by the

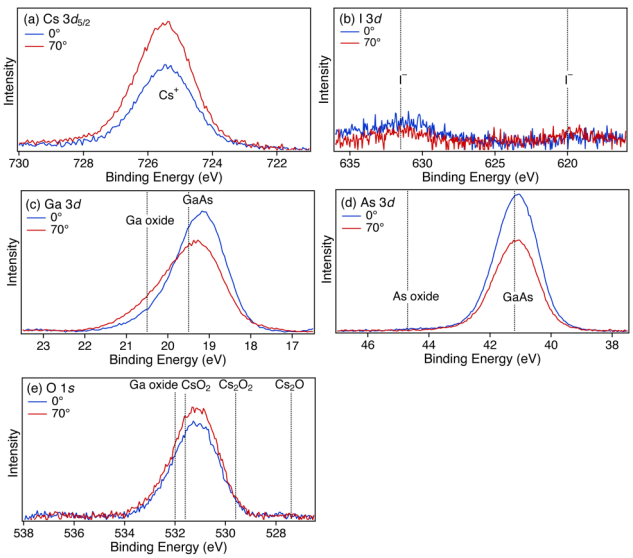

FIG. 9. X-ray photoelectron spectra of CsI/GaAs after heating at 600 °C for 6 h observed with normal (0°, blue) and glancing (70°, red) detection, displaying the (a) Cs $3d_{5/2}$, (b) I 3*d*, (c) Ga 3*d*, (d) As 3*d*, and (e) O 1*s* transitions. Vertical dotted lines represent the nominal binding energies of the labeled species.

spectra in Fig. 10. These spectra were normalized to the maximum intensity of the As 3*d* transition observed in normal detection. This normalization corrected for small, run-to-run changes in alignment and x-ray flux, enabling maximum sensitivity to subtle changes induced by gas exposure.

No systematic changes in the cesium suboxide coating were observed up to the largest exposure of 625 L of both O_2 and H_2O. Subtle, non-systematic changes in the degree of oxidation in the near-surface region were observed, as seen in Fig. 10(c). We attribute these subtle changes to small spatial inhomogeneities in the cesium suboxide coating.

The gas doses probed by this experiment are very large in comparison to those experienced by most photocathodes. For example, a photocathode operated at 10^{-9} Torr would only experience a total gas exposure of 1250 L after more than 14 days of operation.

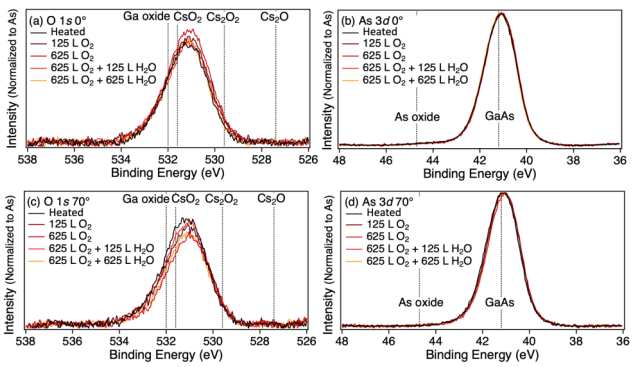

FIG. 10. X-ray photoelectron spectra of heated CsI/GaAs before and after O_2 and H_2O exposure observed with [(a) and (b)] normal (0°) and [(c) and (d)] glancing (70°) detection. The [(a) and (c)] O 1*s* and [(b) and (d)] As 3*d* transitions are shown. Vertical dotted lines represent the nominal binding energies of the labeled species.

VI. DISCUSSION

Heated CsI-coated GaAs and GaN photocathodes activated with Cs or Cs + NF_3 have highly durable activation layers that degrade at a slower rate than photocathodes activated only with Cs or Cs + NF_3, as shown in Figs. 1, 2, and 5. This stability enhancement also requires less cesiation time; about half of the usual cesium dose is required for the activation of initially CsI-coated photocathodes, shown in Fig. 4. Notably, as indicated in Fig. 6, these Cs suboxide-based activation layers maintain high spin polarization, overcoming a common limitation in alternative activation methods.[21,23] Further, the surface quality remains unaffected, as seen in Fig. 7.

The superior performance of heated CsI-coated GaAs photocathodes is not due to iodine. Heating CsI-coated GaAs at 600 °C removes all iodine, leaving a stable surface of Cs suboxides (and perhaps some Ga oxides) as shown in Fig. 9. This surface is chemically robust; both the cesium suboxide layer and the underlying GaAs resist further oxidation during exposures to large O_2 or H_2O doses at room temperature, as shown in Fig. 10. The chemical stability of the cesium suboxide surface was surprising, as we found that the cesium suboxide coating on a cesium antimonide photocathode was sensitive to few L O_2 exposures and completely destroyed by a 100 L O_2 exposure in a previous work.[49]

Previous researchers have used photoelectron spectroscopy to study the activation of GaAs with Cs and O_2, leading to wide agreement that activation produces cesium suboxides. Cs coatings accelerated GaAs oxidation by O_2 by a factor of 10^6 compared to uncoated surfaces in one study.[50] Others showed that GaAs surfaces activated with Cs and O_2 display surface Cs suboxides and oxidized GaAs, indicating that Cs suboxides are a consistent by-product in Cs + O_2 activation layers.[51] The evolution of the Cs suboxide coating across varying activation conditions was studied by others,[52,53] supporting the conclusion that Cs_2O, suboxides and oxidized GaAs typically form on GaAs after Cs + O_2 activation.

If all of these activation schemes lead to cesium suboxide photocathodes, why are the coatings produced from heated CsI/GaAs more robust than others? We suggest that the difference lies in the thermal history of the coating. Previous researchers used Cs metal (Cs^0) sources; however, Cs, which has a melting point of 28 °C, is quite volatile at room temperature. A monolayer of Cs has a calculated lifetime of only 14 s at room temperature.[49,54] Because of this, activation with Cs metal is typically accomplished with multiple sequential Cs and O_2 or NF_3 doses at room temperature. In contrast, CsI is stable at room temperature and does not melt until 632 °C. As a result, our cesium suboxides were produced at significantly higher temperatures. In other words, CsI is a higher

temperature Cs source that leads to films of improved chemical resistance. Additionally, CsI-treated GaAs requiring much less Cs to activate to NEA could be indicative of a work-functioning lowering effect already in place via the Cs-suboxide rich surface.

While these findings are promising, further optimization of CsI layer thickness may enhance performance. While 600 °C has been shown to be an optimal temperature for GaAs photocathode heating,[55] examining variations in heating time and temperature on CsI-based activations may be of value. Performing chemical analysis on samples that have been activated and transported under continuous vacuum could provide additional insight while removing the possibility of contamination during air exposure. The different QEs observed in Fig. 4 may also highlight the need to perform all activations and analysis in the same vacuum chamber, as transport may have created less than ideal NEA conditions. Additional *in-situ* chemical analysis during activation might provide additional insights into the mechanisms behind these lifetime improvements. Further, a residual gas composition analysis of the activation chamber after a lifetime measurement could be used to understand the effects of chemical poisoning as well. Testing the photocathodes in high-current environments is also essential to assess real-world behavior to deleterious effects, such as ion backbombardment. This type of analysis is crucial for the determination of long-term stability and performance under operational conditions.

VII. CONCLUSION

Photocathodes used for the generation of spin-polarized electron beams, such as GaAs and GaN, require a Cs-based activation layer for efficient operation, which typically renders these materials highly susceptible to chemical contamination, significantly limiting their operational lifetimes. In this study, we present a method for extending the dark lifetime of cesium-activated GaN and GaAs photocathodes by applying a cesium iodide (CsI) layer. We show an order-of-magnitude dark lifetime improvement in a GaAs photocathode with the inclusion of a heated CsI layer in the activation process. The underlying mechanisms for this enhancement are examined through XPS and AFM analysis. We found that the heating process removes all the iodine from the surface, leaving only Cs suboxides, which may enhance the chemical robustness of the photocathodes.

ACKNOWLEDGMENTS

The authors thank L. Cultrera, B. D. Dickensheets, S. Kriske, M. W. Olszewski, N. Otto, and B. Vareskic for experimental assistance. This work is supported by United States Department of Energy (DOE) under Grant No. DE-SC0021002 and by the U.S. National Science Foundation under Award No. PHY-1549132, the Center for Bright Beams.

AUTHOR DECLARATIONS

Conflict of Interest

The authors have no conflicts to disclose.

Author Contributions

S. J. Levenson: Data curation (lead); Formal analysis (lead); Writing – original draft (lead); Writing – review & editing (lead). **M. B. Andorf:** Data curation (lead); Formal analysis (equal); Writing – original draft (equal); Writing – review & editing (equal). **M. A. Reamon:** Data curation (supporting); Formal analysis (supporting). **I. V. Bazarov:** Conceptualization (equal); Funding acquisition (equal); Writing – review & editing (equal). **A. Galdi:** Conceptualization (supporting); Formal analysis (supporting); Writing – review & editing (equal). **Q. Zhu:** Data curation (equal); Formal analysis (equal); Writing – review & editing (equal). **M. A. Hines:** Conceptualization (equal); Formal analysis (equal); Funding acquisition (equal); Writing – original draft (equal); Writing – review & editing (equal). **J. Encomendero:** Data curation (supporting). **V. V. Protasenko:** Data curation (supporting). **D. Jena:** Conceptualization (supporting); Funding acquisition (supporting). **H. G. Xing:** Conceptualization (supporting); Funding acquisition (supporting); Writing – review & editing (equal). **J. M. Maxson:** Conceptualization (lead); Funding acquisition (lead); Writing – review & editing (equal).

DATA AVAILABILITY

The data that support the findings of this study are available from the corresponding author upon reasonable request.

REFERENCES

[1]P. Adderley, D. Bullard, Y. Chao, C. Garcia, J. Grames, J. Hansknecht, A. Hofler, R. Kazimi, J. Musson, C. Palatchi, K. Paschke, M. Poelker, G. Smith, M. Stutzman, R. Suleiman, and Y. Wang, "An overview of how parity-violating electron scattering experiments are performed at CEBAF," Nucl. Instrum. Methods Phys. Res., Sect. A **1046**, 167710 (2023).
[2]S. Heidrich, K. Aulenbacher, M. Bruker, M. Dehn, and P. Heil, "High-current emittance measurements at MAMI," in *Proceedings of IPAC'19, Melbourne, Australia, May 2019* (JACoW Publishing, Geneva, Switzerland, 2019), pp. 4121–4123.
[3]S. Michizono, "The International Linear Collider," Nat. Rev. Phys. **1**, 244–245 (2019).
[4]D. Xu, E.-C. Aschenauer, G. Bassi, J. Beebe-Wang, J. Berg, W. Bergan, M. Blaskiewicz, A. Blednykh, J. Brennan, S. Brooks, K. Brown, Z. Conway, K. Drees, A. Fedotov, W. Fischer, C. Folz, D. Gassner, X. Gu, R. Gupta, and J. Unger, "EIC beam dynamics challenges," in *Proceedings of the 13th International Particle Accelerator Conference* (JACoW Publishing, Geneva, Switzerland, 2022), p. WEIXGD1.
[5]M. Suzuki, M. Hashimoto, T. Yasue, T. Koshikawa, Y. Nakagawa, T. Konomi, A. Mano, N. Yamamoto, M. Kuwahara, M. Yamamoto, S. Okumi, T. Nakanishi, X. Jin, T. Ujihara, Y. Takeda, T. Kohashi, T. Ohshima, T. Saka, T. Kato, and H. Horinaka, "Real time magnetic imaging by spin-polarized low energy electron microscopy with highly spin-polarized and high brightness electron gun," Appl. Phys. Express **3**, 026601 (2010).
[6]M. Kuwahara, S. Kusunoki, Y. Nambo, K. Saitoh, X. Jin, T. Ujihara, H. Asano, Y. Takeda, and N. Tanaka, "Coherence of a spin-polarized electron beam emitted from a semiconductor photocathode in a transmission electron microscope," Appl. Phys. Lett. **105**, 193101 (2014).
[7]N. Rougemaille and A. Schmid, "Magnetic imaging with spin-polarized low-energy electron microscopy," Eur. Phys. J. Appl. Phys. **50**, 20101 (2010).
[8]D. Pierce and F. Meier, "Photoemission of spin-polarized electrons from GaAs," Phys. Rev. B **13**, 5484 (1976).

[9]D. Pierce, R. Celotta, G. Wang, W. Unertl, A. Galejs, and C. Kuyatt, "The GaAs spin polarized electron source," Rev. Sci. Instrum. **51**, 478–499 (1980).
[10]S. Karkare, L. Boulet, A. Singh, R. Hennig, and I. Bazarov, "Ab initio studies of Cs on GaAs (100) and (110) surfaces," Phys. Rev. B **91**, 035408 (2015).
[11]G. Bir, A. Aronov, and G. Pikus, "Spin relaxation of electrons due to scattering by holes," Sov. Phys.-JETP **42**, 705 (1976).
[12]M. D'Yakonov and V. Perel, "Spin orientation of electrons associated with the interband absorption of light in semiconductors," Sov. Phys.-JETP **33**, 1053 (1971).
[13]R. Elliott, "Theory of the effect of spin-orbit coupling on magnetic resonance in some semiconductors," Phys. Rev. **96**, 266 (1954).
[14]O. Chubenko, S. Karkare, D. A. Dimitrov, J. K. Bae, L. Cultrera, I. Bazarov, and A. Afanasev, "Monte Carlo modeling of spin-polarized photoemission from p-doped bulk GaAs," J. Appl. Phys. **130**, 063101 (2021).
[15]T. Maruyama, E. Garwin, R. Prepost, and G. Zapalac, "Electron-spin polarization in photoemission from strained GaAs grown on $GaAs_{1-x}P_x$," Phys. Rev. B **46**, 4261 (1992).
[16]N. Chanlek, J. D. Herbert, R. M. Jones, L. B. Jones, K. J. Middleman, and B. L. Militsyn, "The degradation of quantum efficiency in negative electron affinity GaAs photocathodes under gas exposure," J. Phys. D: Appl. Phys. **47**, 055110 (2014).
[17]T. Wada, T. Nitta, T. Nomura, M. Miyao, and M. Hagino, "Influence of exposure to CO, CO_2 and H_2O on the stability of GaAs photocathodes," Jpn. J. Appl. Phys. **29**, 2087 (1990).
[18]I. Petrushina *et al.*, "Superconducting RF gun with high current and the capability to generate polarized electron beams," in *12th International Particle Accelerator Conference* (JACoW Publishing, Geneva, Switzerland, 2021).
[19]J. Bae, L. Cultrera, P. Digiacomo, and I. Bazarov, "Rugged spin-polarized electron sources based on negative electron affinity GaAs photocathode with robust Cs_2Te coating," Appl. Phys. Lett. **112**, 154101 (2018).
[20]J. Biswas, E. Wang, M. Gaowei, W. Liu, O. Rahman, and J. T. Sadowski, "High quantum efficiency GaAs photocathodes activated with Cs, O_2, and Te," AIP Adv. **11**, 025321 (2021).
[21]L. Cultrera, A. Galdi, J. K. Bae, F. Ikponmwen, J. Maxson, and I. Bazarov, "Long lifetime polarized electron beam production from negative electron affinity GaAs activated with Sb-Cs-O: Trade-offs between efficiency, spin polarization, and lifetime," Phys. Rev. Accel. Beams **23**, 023401 (2020).
[22]J. K. Bae, M. Andorf, A. Bartnik, A. Galdi, L. Cultrera, J. Maxson, and I. Bazarov, "Operation of Cs–Sb–O activated GaAs in a high voltage DC electron gun at high average current," AIP Adv. **12**, 095017 (2022).
[23]J. K. Bae, A. Galdi, L. Cultrera, F. Ikponmwen, J. Maxson, and I. Bazarov, "Improved lifetime of a high spin polarization superlattice photocathode," J. Appl. Phys. **127**, 124901 (2020).
[24]L. Cultrera, "Spin polarized electron beams production beyond III-V semiconductors," arXiv:2206.15345 (2022).
[25]V. Rusetsky, V. Golyashov, S. Eremeev, D. Kustov, I. Rusinov, T. Shamirzaev, A. Mironov, A. Demin, and O. Tereshchenko, "New spin-polarized electron source based on alkali antimonide photocathode," Phys. Rev. Lett. **129**, 166802 (2022).
[26]S. J. Levenson, M. B. Andorf, B. D. Dickensheets, I. V. Bazarov, A. Galdi, J. Encomendero, V. V. Protasenko, D. Jena, H. G. Xing, and J. M. Maxson, "Measurement of spin-polarized photoemission from wurtzite and zinc blende gallium nitride photocathodes," Appl. Phys. Lett. **125**, 034107 (2024).
[27]T. Nishitani, M. Tabuchi, H. Amano, T. Maekawa, M. Kuwahara, and T. Meguro, "Photoemission lifetime of a negative electron affinity gallium nitride photocathode," J. Vac. Sci. Technol. B **32**, 06F901 (2014).
[28]T. Boutboul, A. Akkerman, A. Breskin, and R. Chechik, "Escape length of ultraviolet induced photoelectrons in alkali iodide and CsBr evaporated films: Measurements and modeling," J. Appl. Phys. **84**, 2890–2896 (1998).
[29]T. Boutboul, A. Akkerman, A. Gibrekhterman, A. Breskin, and R. Chechik, "An improved model for ultraviolet- and x-ray-induced electron emission from CsI," J. Appl. Phys. **86**, 5841–5849 (1999).
[30]E. Shefer, A. Breskin, T. Boutboul, R. Chechik, B. K. Singh, H. Cohen, and I. Feldman, "Photoelectron transport in CsI and CsBr coating films of alkali antimonide and CsI photocathodes," J. Appl. Phys. **92**, 4758–4771 (2002).
[31]A. Akkerman, T. Boutboul, A. Breskin, R. Chechik, and A. Gibrekhterman, "Low-energy electron transport in alkali halides," J. Appl. Phys. **76**, 4656–4662 (1994).
[32]B. Singh, E. Shefer, A. Breskin, R. Chechik, and N. Avraham, "CsBr and CsI UV photocathodes: New results on quantum efficiency and aging," Nucl. Instrum. Methods Phys. Res., Sect. A **454**, 364–378 (2000).
[33]E. Taft and H. Philipp, "Photoelectric emission from the valence band of some alkali halides," J. Phys. Chem. Solids **3**, 1–6 (1957).
[34]E. Nappi, "CsI RICH detectors in high energy physics experiments," Nucl. Instrum. Methods Phys. Res., Sect. A **471**, 18–24 (2001).
[35]A. Mauro, P. Martinengo, F. Piuz, E. Schyns, J. van Beelen, and T. Williams, "Study of the quantum efficiency of CsI photo-cathodes exposed to oxygen and water vapour," Nucl. Instrum. Methods Phys. Res., Sect. A **461**, 584–586 (2001), 8th Pisa Meeting on Advanced Detectors.
[36]Y. Xie, A. Zhang, Y. Liu, H. Liu, T. Hu, L. Zhou, X. Cai, J. Fang, B. Yu, Y. Ge, Q. Lü, X. Sun, L. Sun, Z. Xue, Y. Xie, Y. Zheng, and J. Lü, "Influence of air exposure on CsI photocathodes," Nucl. Instrum. Methods Phys. Res., Sect. A **689**, 79–86 (2012).
[37]L. Kong, A. G. Joly, T. C. Droubay, and W. P. Hess, "Quantum efficiency enhancement in CsI/metal photocathodes," Chem. Phys. Lett. **621**, 155–159 (2015).
[38]V. Vlahos, D. Morgan, and J. H. Booske, "Material analysis and characterization of cesium iodide (CsI) coated C fibers for field emission applications," in *2008 IEEE 35th International Conference on Plasma Science, Karlsruhe, Germany* (IEEE, 2008), pp. 1.
[39]R. Fukuoka, K. Ezawa, Y. Koshiba, K. Sakaue, and M. Washio, "Study on the performance improvement of alkali antimonide photocathodes for radio frequency electron guns," in *Proceedings of IPAC'22, International Particle Accelerator Conference No. 13, Geneva, Switzerland* (JACoW Publishing, 2022), pp. 2640–2642.
[40]K. Ezawa, R. Fukuoka, Y. Koshiba, K. Sakaue, T. Tamba, and M. Washio, "Study on durability improvement of Cs-Te Photocathode by means of alkali halide protective films," in *Proceedings of IPAC'21, Geneva, Switzerland* (JACoW Publishing), pp. 2847–2849.
[41]S. Levenson, M. Andorf, I. Bazarov, J. Encomendero, D. Jena, J. Maxson, V. Protasenko, and H. Xing, "Characterization of various GaN samples for photoinjectors," in *Proc. 13th International Particle Accelerator Conference (IPAC'22), International Particle Accelerator Conference No. 13, Geneva, Switzerland* (JACoW Publishing, 2022), pp. 500–502.
[42]L. Cultrera *et al.*, "Photocathodes R&D for high brightness and highly polarized electron beams at Cornell University," in *Proceedings of IPAC'18* (JACoW Publishing, Geneva, Switzerland, 2018), pp. 1601–1604.
[43]M.-G. Kang, S.-H. Sa, H.-H. Park, K.-S. Suh, and Kyung-Hui Oh, "The characterization of etched GaAs surface with HCl or H_3PO_4 solutions," Thin Solid Films **308–309**, 634–642 (1997).
[44]H. Araghi-Kozaz, G. Brojerdi, M. Besancon, P. Dolle, and J. Jupille, "The role of a superoxo-like species in the oxidation of alkali metal-precovered GaAs (100) surfaces," Surf. Sci. **251/252**, 1091–1095 (1991).
[45]J. Hrbek, Y. W. Yang, and J. A. Rodriguez, "Oxidation of cesium multilayers," Surf. Sci. **296**, 164–170 (1993).
[46]S. W. Gaarenstroom and N. Winograd, "Initial and final state effects in the ESCA spectra of cadmium and silver oxides," J. Chem. Phys. **67**, 3500–3506 (1977).
[47]C. Y. Su, I. Lindau, P. W. Chye, P. R. Skeath, and W. E. Spicer, "Photoemission studies of the interaction of oxygen with GaAs (110)," Phys. Rev. B **25**, 4045–4068 (1982).
[48]J. Jupille, P. Dolle, and M. Besancon, "Ionic oxygen species formed in the presence of lithium, potassium and cesium," Surf. Sci. **260**, 271–285 (1992).
[49]A. Galdi, W. J. I. DeBenedetti, J. Balajka, L. Cultera, I. V. Bazarov, J. M. Maxson, and M. A. Hines, "The effects of oxygen-induced phase segregation on the interfacial electronic structure and quantum efficiency of Cs_3Sb photocathodes," J. Chem. Phys. **153**, 144705 (2020).

[50]C. Y. Su, P. W. Chye, P. Pianetta, I. Lindau, and W. E. Spicer, "Oxygen adsorption on Cs covered GaAs (110) surfaces," Surf. Sci. **86**, 894–899 (1979).
[51]G. Faraci, A. R. Pennisi, and G. Margaritondo, "Catalytic oxidation of the GaAs (110) surface promoted by a Cs overlayer," Phys. Rev. B **53**, 13851–13856 (1996).
[52]J. X. Wu, F. Q. Li, J. S. Zhu, M. R. Ji, and M. S. Ma, "Annealing behavior of a Cs_2O/Cs_2O_2/GaAs (110) surface studied by electron spectroscopy," J. Vac. Sci. Technol. A **20**, 1532–1535 (2002).
[53]J. Biswas, J. Cen, M. Gaowei, O. Rahman, W. Liu, X. Tong, and E. Wang, "Revisiting heat treatment and surface activation of GaAs photocathodes: In-situ studies using scanning tunneling microscopy and photoelectron spectroscopy," J. Appl. Phys. **128**, 045308 (2020).
[54]A. W. Grant and C. T. Campbell, "Cesium adsorption on TiO_2(110)," Phys. Rev. B **55**, 1844–1851 (1997).
[55]N. Chanlek, J. D. Herbert, L. B. Jones, R. M. Jones, and K. J. Middleman, "A study of the activated gaas surface for application as an electron source in particle accelerators," AIP Conf. Proc. **1149**, 1022–1026 (2009).